The observation of spectral lines from ions of fast oxygen injected into the TJ-II stellarator during neutral beam heating

K. J. McCarthy, J. Arévalo, V. Tribaldos, J.M. Fontdecaba, and TJ-II team

Laboratorio Nacional de Fusión, Asociación EURATOM-CIEMAT, E-28040 Madrid, Spain

Introduction

TJ-II is a four-period stellarator of the heliac type with a major radius of 1.5 m, a bean shaped plasma cross-section with an average minor radius of ≤0.22 m, and magnetic field B(0) ≤1 T designed to explore a wide rotational transform range ($0.9 \leq \iota(0)/2\pi \leq 2.2$) in low, negative shear configurations ($\Delta\iota/\iota$ <6%) [1]. Plasmas created with hydrogen are heated using two gyrotrons operated at 53.2 GHz, the 2nd harmonic of the electron cyclotron resonance frequency (P_{ECRH} ≤600 kW, t ≤300 ms) and central electron densities, $n_e(0)$, and temperatures, $T_e(0)$, up to 1.7×10^{19} m^{-3} and 2 keV, are attained. TJ-II is the first heliac device to employ neutral beams for additional heating. At present, two such injectors (NBI's) provide up to ~1 MW (E ≤32 keV) for ≤100 ms. As a result plasmas with $n_e(0) \leq 5\times10^{19}$ m^{-3} have been attained. This system is comprised of two tangential injectors in the 'Co'-'Counter' configuration [2]. See Fig. 1. Each consists of an arc discharge source, acceleration grids, a neutralization chamber and ion dump. The cold dense plasma generated in the anodes (~10^{14} H_2 cm^{-3}, T_e = 5 eV) is composed principally of H^+ and electrons with a not insignificant presence of molecular ions, *i.e.* H_2^+, H_3^+. The composition depends on the arc conditions, the theoretical ion species mix being 80:10:10% (H^+, H_2^+, H_3^+). However, impurities are also present in the source. Accelerated impurities ions (*e.g.* H_2O^+, H_3O^+) undergo the same accelerating, disassociation and neutralization processes so their neutral particles exit with energies mE/M where m and M are the atomic masses of the resulting neutral particles and original impurity ions, respectively. Indeed, a low energy component is observed among the Doppler shifted H_α spectral lines from TJ-II neutral beams. See Fig. 2. Finally, all accelerated neutrals pass penetrate into the hot plasmas where they can be ionized, in collisions with protons and impurity ions, and become trapped.

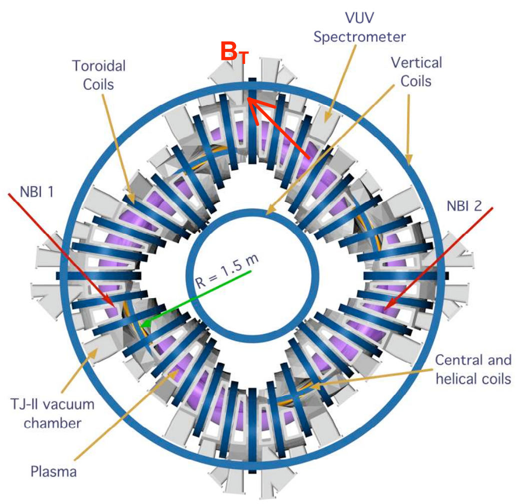

Fig. 1: Bird's eye view of the TJ-II

The TJ-II is equipped with numerous modern diagnostics including a VUV spectrometer.

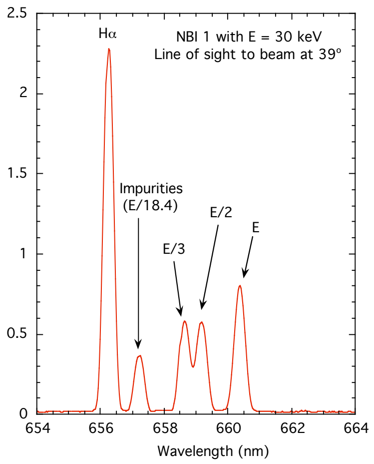

Fig. 2: Doppler shifted Hα emissions from the NBI#1 neutral beam

Time resolved spectral line information is collected in survey mode every 5 ms using an f/10.4 1 m normal-incidence spectrometer. This instrument, which covers the range from 20 to 300 nm, is mounted with its wavelength dispersion plane perpendicular to the central conductor and located in a sector where its line-of-sight does not intercept either NBI beam path. See Fig. 1. Moreover, because of helicity, the angles γ between the line-of-sight and magnetic field line vectors are <90°, *e.g.* $\gamma \sim 55°$ for the standard magnetic configuration, so spectral lines are shifted by poloidal and toroidal velocity components. For this work the viewing solid angle was restricted by stops to collect radiation from 10 cm of the plasma cross-section (about the central magnetic axis) plus a few centimetres in the toroidal direction.

Observed Spectral Features

Broad line-like spectral features were first observed about the O V resonance line at 62.97 nm ($2s^2\ ^1S$ - $2s2p\ ^1P^o$) during NBI heating where their intensities reaching up to 10% that of the main peak while their temporal evolution did not correlate with main plasma parameters. See Fig. 3. Also, their full-widths at half-maximum (FWHM), ~0.065 nm, implied ion temperatures significantly higher than impurity temperatures typically measured in TJ-II, *i.e.* 50 to 200 eV [3]. Moreover, it was found that when NBI#1 was operated, the feature appeared on the short wavelength side of the line, whilst when NBI#2 was operated, the feature appeared on its long wavelength side. Finally, when both NBI's were operated the features were present on both sides of the line (albeit asymmetrically), and disappeared several milliseconds after NBI switch-off.

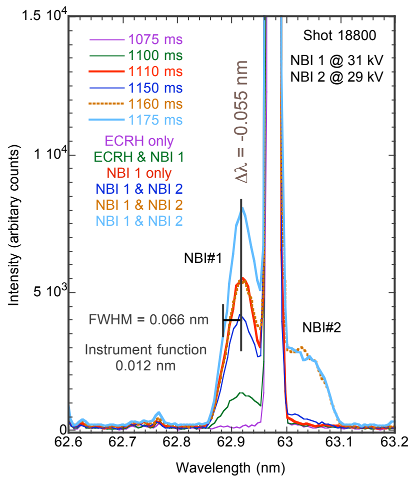

Fig 3: Features appear on the short and long wavelength sides of the O V line at 62.97 nm during NBI heating

Similar features were found about other strong lines emitted by various ionization states of oxygen, for instance, about the 59.78 and 59.96 nm ($2p^2\ ^1D - 2p^3\ ^1D^o$) lines of O III, the 60.84 and 60.98 nm ($2p\ ^2P^o - 2p^2\ ^2S$) lines of O IV as well as its resonance lines at 78.77, 79.01 and 79.02 nm ($2p\ ^2P^0 - 2p^2\ ^2D$), and the resonance O VI lines at 103.19 nm and 103.76 nm ($2s\ ^2S$ -

2p $^2P^o$). See Figs. 4. In all cases after crosschecking with atomic spectra database, it was ascertained that their wavelengths did not coincide with those of known TJ-II impurities. In contrast, due to the large number of closely spaced lines, it was not possible to determine if structures occurred about the strong O II lines at 83.27, 83.33 and 83.45 nm ($2p^3\ ^4S^0$ - $2p^4\ ^4P$) or about the resonance O III lines at 83.5 nm ($2p^2\ ^3P$ - $2p^3\ ^3D^o$). Finally, features were not observed about spectral lines from higher ionization states of oxygen, for instance about the 162.36, 163.83 and 163.99 nm ($2s\ ^3S$ – $2p\ ^3P^o$) lines of O VII nor about transitions of O VIII at 29.28 nm and 63.265 nm, respectively, all of which are tenuous or not observed in TJ-II plasmas.

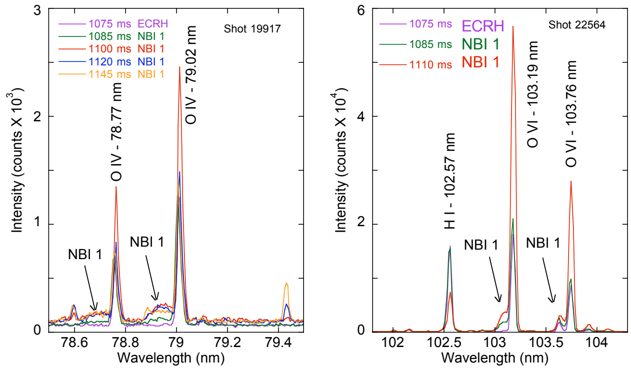

Fig. 4 Features appear on the short wavelength sides of O IV (79 nm) and O VI (103 nm) lines during NBI#1 heating.

Discussion

Now considering the above, plus the presence of accelerated oxygen in the NBI's, it is considered that the structures are line emissions from fast neutral oxygen ions that enter the plasma as neutrals with energy mE/M and velocity V (m/s) = $1.3\times10^2\ (1.16\times10^4\ E/M)^{0.5}$, become ionized by collisions and charge exchange with protons, are trapped by the magnetic field, and then undergo further ionizations (with little or no slowing down) as they follow the magnetic field lines (in a cork screw manner) around the TJ-II. Also, these ions remain in the plasma for sufficient time for line emissions, induced by collisional excitation, to be observed in the spectrometer which is well removed from the initial ionization positions.

In the first instance, the ionization cross-section for fast oxygen, σ_Σ, is similar to that for fast hydrogen (5-6 $\times10^{-16}$ cm^{-2}) [4], hence a comparable or higher trapping rate can be assumed. Here σ_Σ includes collisional ionization ~10^{-16} cm^2 [5]) and charge-exchange (4-5 $\times\ 10^{-16}$ cm^2 [6]) by plasma ions plus transfer ionization (3-4 $\times\ 10^{-17}$ cm^2 [7]). Moreover, as density increases towards the plasma centre, trapping is maximized in the core, *i.e.* ions trapped close to the edge may enter the loss cone and be expelled. Similarly, trapping will also increase when density increases with NBI heating. Now, the velocity vector of the ionized oxygen will be modified as $V^2 = V_{par}^2 + V_{per}^2$ ($E = 1/2\ mV_{par}^2 + \mu B_T$ and $\mu = mV_{per}^2 / 2|B_T|$ is magnetic moment) where V_{par} and V_{per}, the velocities of the trapped oxygen travelling along, and gyrating about, magnetic field lines, depend on the angle γ between the toroidal magnetic field, **B**, and the **V** vectors at ionization. However, since injection is tangential, γ will be small in the core and $V_{par} \approx V$. Thus oxygen ions follow the magnetic field lines (in a cork screw manner) around TJ-II. From NBI#1, they travel in an anti-clockwise direction (seen from above in Fig. 1) following the magnetic field lines as they twist around the central coil. In contrast, ions originating from NBI#2 travel clockwise.

Following the above discussion, the trapped oxygen ions undergo further ionization as they follow the magnetic field lines. For instance, at NBI switch-on, when $n_e(0) < 10^{19}$ m^{-3}, $T_e(0)$ ~800 eV, $Z_{eff} = 2$, and $T_i(0)$ ~80 eV, the mean times for ionization (with respect to the initial ionization) to $O^{+3,}$ O^{+4}, O^{+5}, and O^{+6} are ~9, ~25, ~60 and ~160 μs respectively (these are determined for electron collisional ionization [8]). Now, during these same times O^{+q} ions, for $q \geq 3$, can reach the VUV spectrometer sector C6 (note: the path lengths around TJ-II from NBI#1 and from NBI#2 to C6 are 6.7 m and 8.5 m, respectively, and excitation is assumed local *i.e.*, $A_{ki} > 10^8$ s^{-1}). Moreover, for these plasma conditions, the slowing down times for these ions will be of the order of milliseconds or longer, hence the initial V_{par} and V_{per} will not alter. Otherwise, a skewed 'slowing-down' function would be expected. Thus spectral lines collected by the spectrometer will display Doppler shifts of the order +/- $\lambda_0 V_{par} \text{Cos}\, \psi / c$, where c is the speed of light and λ_0 is the rest wavelength. Moreover, as there exists a range of γ's for initial ionizations, V_{par} will have a velocity distribution which would explain the feature broadening. Indeed, broadening by a distribution in the gyrating component, V_{per}, should also be considered. Finally, the shape of the feature is seen to be dependent on the direction of B_T. When inverted the line shapes about the main oxygen line are seen to swap over. This may be due to shifting of the stagnation point with respect to the magnetic surfaces. This being outwards if the fast ions are injected parallel to the toroidal current (co-injection) and inwards for the opposite (counter-injection). More, investigation is needed to clarify this.

Acknowledgements

This work is partially financed by the Spanish *Ministerio de Ciencia e Innovación*, Ref. FTN2007-64159.

References

[1] C. Hidalgo *et al.*, Nucl. Fusion, 45 (2005), S266.

[2] M. Liniers *et al.*, Vacuum 67 (2002) 379.

[3] J. M. Carmona *et al.*, Fusion Sci. Tech. 54, (2008) 962.

[4] E. Speth, Rep. Prog. Phys. 52 (1989) 57.

[5] W.R. Thompson *et al.*, J. Phys. B: At. Mol. Opt. Phys. 30 (1997) L207.

[6] W.R. Thompson et *al.*, J. Phys. B: At. Mol. Opt. Phys. 28 (1995) 1321.

[7] W.R. Thompson et *al.*, J. Phys. B: At. Mol. Opt. Phys. 29 (1996) 725.

[8] Y. Itikawa *et al.*, At. Data Nucl. Data Tables 33 (1985) 149.